

Structure and Mass Distribution of the Milky Way Bulge and Disk

Ortwin Gerhard

*Astronomisches Institut, Universität Basel,
Venusstr. 7, CH-4102 Binningen, Switzerland*

Abstract. This article summarizes the structural parameters of the Galactic bulge and disk, and discusses the interpretation of the bulge microlensing observations and the determination of the Milky Way's luminous mass from the terminal velocity curve and the Oort limit. The bulge is a rotating bar with corotation radius around 4 kpc. The NIR disk has a short scale-length. The measured surface density of the local disk is in good agreement with the prediction of a maximum NIR disk model for the Milky Way. The preliminary new value for the microlensing optical depth of clump giant sources is within 1.7σ of the prediction by the maximum NIR disk model, while the optical depth for all sources is still significantly higher. These results imply that cold dark matter cannot dominate inside the solar radius.

1. Introduction

The Milky Way is a normal galaxy seen under a magnifying glass: the ages, metallicities, and kinematics of its stars can be observed in much greater detail than in any other galaxy. Combined with a model for the large-scale structure and potential, dynamical models for specific stellar populations can be constructed which link our local neighbourhood with distant parts of the Galaxy. Thus we can study in a unique way the imprints of the evolution and formation processes that shaped the Milky Way, and presumably other galaxies as well.

As is well-known, our viewpoint from within the Galactic disk also has some drawbacks, in that many of the Milky Way's large scale properties have been difficult to obtain. Only in the last decade has it become possible to map the old stellar population in the Galactic bulge and inner disk, using infrared observations to penetrate the dust layers in the disk. Models are needed to interpret these data and link them to gas kinematical and other observations. Two important results are that the inner Galaxy contains a rotating bar/bulge, and that the scale-length of the disk is significantly shorter than previously assumed.

Microlensing surveys have now found hundreds of events towards the Galactic bulge. From such data and from local stellar-kinematic measurements, direct constraints on the mass of the Milky Way's bulge and disk can be obtained, which are difficult to come by in external galaxies, and which can be used to test cosmological models of dark matter halo and galaxy formation.

2. Structure of the Galactic bulge and disk

The best evidence for a rotating bar in the inner Galaxy comes from maps of the NIR light distribution, from star counts along various lines-of-sight, from the non-circular motions observed in the atomic and molecular gas, and from the large optical depth to microlensing towards the bulge. For a more extensive review than given here see Gerhard (1999, G99). All length scales given below are for a Sun-center distance $R_0 = 8$ kpc.

Several models for the distribution of old stars in the inner Galaxy have been based on the COBE/DIRBE NIR data. These data have complete sky coverage but relatively low spatial resolution, they must still be ‘cleaned’ for residual dust absorption, and they contain no distance information, so deprojection is not straightforward. The cleaned data show that the bulge is brighter and more extended in latitude b at positive longitudes l than at corresponding $-l$, except for a region close to the center where the effect is reversed (Weiland *et al.* 1994, Bissantz *et al.* 1997). The asymmetry is strongest around $|l| \simeq 10^\circ$. These signatures are as expected for a barred bulge with its long axis in the first quadrant (Blitz & Spergel 1991). The region of reversed asymmetry at small $|l|$ argues for a bar rather than a lopsided light distribution; see also Sevenster (1999).

Dwek *et al.* (1995) and Freudenreich (1998) fitted parametric models to the cleaned DIRBE data, assuming specific functional forms for the barred bulge and excluding low-latitude regions from the fit. In this way the derived outer bulge properties are less likely to be influenced by the disk light, but the inner bulge and disk profiles are ill-determined. Non-parametric models were constructed by Binney, Gerhard & Spergel (1997, BGS), using a Lucy algorithm based on the assumption of strict triaxial symmetry, and by Bissantz & Gerhard (2000), using a penalized maximum likelihood algorithm. The new model by Bissantz & Gerhard includes a spiral arm model and maximizes eightfold symmetry only for the remaining luminosity distribution. In this model the bulge-to-disk ratio in NIR luminosity is about 20%, similar to the value given by Kent, Dame & Fazio (1991). Other bar and disk properties from the COBE models are summarized below. Physical models for the COBE bar can be found for a range of bar orientation angles, $15^\circ \lesssim \varphi_{\text{bar}} \lesssim 35^\circ$, where φ_{bar} measures the angle in the Galactic plane between the bar’s major axis at $l > 0$ and the Sun-center line. φ_{bar} must therefore be determined from other data; see also Zhao (2000).

The bar is also seen in starcount observations in inner Galaxy fields. Stanek *et al.* (1997) analyzed reddening-corrected apparent magnitude distributions of clump giant stars in 12 OGLE fields. The small intrinsic luminosity spread (~ 0.2 - 0.3 mag) makes these stars good distance indicators. The peak of the distribution is brighter at $l > 0$ where the line-of-sight passes through the near side of the bar. These fields cover only a small fraction of the sky, but fitting a parametric model constrains the bar orientation angle as well as the axis ratios and density profile. Nikolaev & Weinberg (1997) reanalyzed the IRAS variable population in a similar spirit; here the distance information comes from the known range of AGB star luminosities. NIR starcounts have also shown longitudinal asymmetries due to the bar (Unavane & Gilmore 1998). López-Corredoira *et al.* (1997, 2000) and Hammersley *et al.* (1999) have modelled the Two Micron Survey Starcounts (mostly bright K and M giants) in several

strips across the bulge. Structural information on the bulge and disk can be derived from these data together with a model for the bright-star luminosity function. Ongoing work on deeper surveys (ISOGAL, DENIS, 2MASS) will provide important new information on the old stellar population in the inner Galaxy; a preview of results is given in van Loon (2000).

Modelling the HI and CO (l, v) diagrams provides information on the gravitational potential of the bar and disk. Several recent gas flow models have followed complementary approaches: Englmaier & Gerhard (1999) modelled the gas flow in the potential of the rotating COBE bar of Binney, Gerhard & Spergel (1997), Fux (1999) determined a best-fitting N-body-SPH model from a sequence of ab initio simulations, and Weiner & Sellwood (1999) considered gas flows in a sequence of analytic model potentials. These simulations produce (l, v) diagrams with which many features seen in the observed (l, v) diagrams may be qualitatively understood, such as the 3 kpc arm, the non-circular velocities around the end of the bar, the cusped-orbit shock transition and inner x_2 -disk, the molecular ring and the spiral arm tangent locations. However, no model as yet provides a satisfactory quantitative account of the Galactic gas disk. A fuller discussion can be found in G99.

The following subsections contain my best summary of the main bar and disk parameters from this and other work.

Corotation radius: This is the most important bar parameter. The gas-dynamical simulations of Englmaier & Gerhard (1999) and Fux (1999) agree in their interpretation of the 3 kpc arm as one of the lateral arms close to the bar, placing it inside corotation. Sevenster (1999) argues that the 3 kpc arm is part of an inner ring, which would also place it slightly inside the corotation radius R_{CR} . The main Galactic spiral arms outside R_{CR} , on the other hand, imply an upper limit for R_{CR} , but this is more model-dependent. The gas-dynamical models thus give a range of $3 \text{ kpc} \lesssim R_{CR} \lesssim 4.5 \text{ kpc}$; a corresponding resonance diagram is shown in G99. Dehnen (2000) has interpreted features in the local stellar velocity distribution as due to the outer Lindblad resonance with the bar, resulting in $R_{CR} = 0.55 \pm 0.05 R_0$, near the upper end of the range from the gas-dynamical models. While the match to the Hipparchos data appears convincing, it is not clear whether and why this way of determining R_{CR} should work, because the bar is too weak to excite the spiral arms between R_{CR} and the solar radius, and these spiral arms should dominate the local quadrupole moment (Englmaier & Gerhard 1999).

Bar orientation From the integrated light alone, physically reasonable models can be found for $15^\circ \lesssim \varphi_{\text{bar}} \lesssim 35^\circ$. Starcount models give values between $\varphi_{\text{bar}} = 12 \pm 6^\circ$ (López-Corredoira *et al.* 2000) and $20 - 30^\circ$ (Nikolaev & Weinberg 1997, Stanek *et al.* 1997). The models of Bissantz & Gerhard (2000) for the DIRBE L-band data, when additionally constrained by the clump giant apparent magnitude distributions of Stanek *et al.* (1997), give an optimal $\varphi_{\text{bar}} = 15^\circ$ (Figure 1), but $\varphi_{\text{bar}} \simeq 15 - 25^\circ$ is within the uncertainties. The gas-dynamical models and the orbit analysis of Binney *et al.* (1991) are also compatible with $15^\circ \lesssim \varphi_{\text{bar}} \lesssim 35^\circ$, depending on whether the emphasis is on the peak in the terminal velocity curve, the arm morphology, or the magnitude of the non-circular motions near the 3 kpc arm. Finally, microlensing observations favour $\varphi_{\text{bar}} \sim 15^\circ$ (Zhao & Mao 1996, §3). Thus a good working value is $\varphi_{\text{bar}} = 20^\circ$.

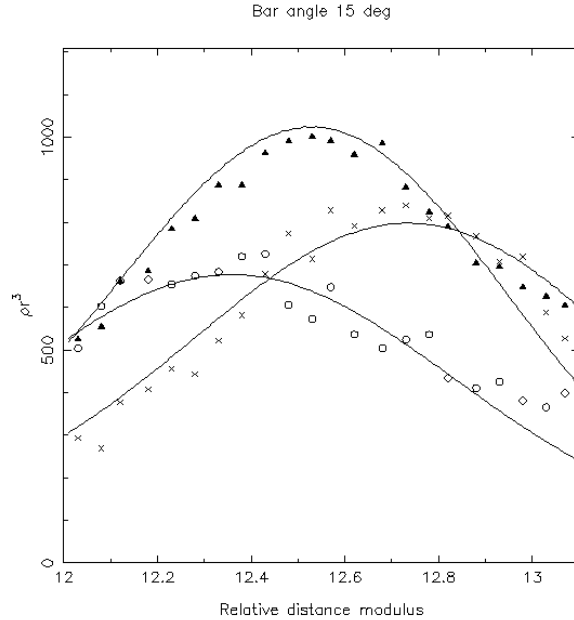


Figure 1. Apparent magnitude distribution of clump giant stars in three fields observed by Stanek *et al.* (1997) with superposed scaled model predictions from Bissantz & Gerhard (2000) for their model with $\varphi_{\text{bar}} = 15^\circ$. The model curves have been normalized and shifted along the abscissa such that the $l = 5.5^\circ$ and $l = -4.9^\circ$ peaks match best the locations of the observed peaks (circles and crosses, respectively). Note that the relative number, width, and asymmetry of the observed distributions in these fields and in Baade's window (triangles) are matched well.

Not consistent with this appear to be the bar model of Hammersley *et al.* (2000), which is based on the identification of a region of strong star formation at $l = 27^\circ$ with the nearer end of the bar, and the star count results reported in van Loon (2000), which place the near end of a 1.4 kpc size bar at negative longitudes.

Bar length: Models based on the DIRBE NIR maps find the end of the bar around $R_{GC} = 3.2 \pm 0.3$ kpc, when $\varphi_{\text{bar}} \simeq 20^\circ$ (Freudenreich 1998, BGS, Bissantz & Gerhard 2000). This is consistent with with the OH/IR stars (Sevenster 1999), IRAS variables (Nikolaev & Weinberg 1997), and the range of R_{CR} above for a fast bar, while other starcount models use exponential or Gaussian density distributions with shorter scale-lengths.

Bar axis ratios: The parametric DIRBE models give axial ratios of about 10:3-4:3. This is in agreement with the new non-parametric model of Bissantz & Gerhard (2000), whereas BGS had found 10:6:4 without taking into account the spiral arms. The starcount models give 10:4:3 (Stanek *et al.* 1997) and 10:5.4:3.3 (López-Corredoira *et al.* 2000). Thus there is good overall agreement at around 10:4:3.

Disk scale-length: In the integrated NIR the radial exponential disk scale R_D is significantly shorter than in the optical; numerical values are around 2.5 kpc (Freudenreich 1998, BGS) or somewhat shorter (2.1 kpc, Bissantz & Gerhard

2000). Hammersley *et al.* (1999) report satisfactory agreement of their NIR counts with a model with $R_d = 3.5$ kpc, but have not tested other values of R_D . López-Corredoira *et al.* (2000) find that $R_d = 3.0$ kpc is too short to describe the NIR TMSS counts well. Earlier starcount models (Robin *et al.* 1992, Ortiz & Lépine 1993) favour a short disk scale, $R_d = 2.5$ kpc. It is not clear what causes the differences between the various starcount models, and between the TMSS starcounts and the integrated NIR light. There may be some interplay between the disk scale-length, the bulge profile, and the spiral arm luminosity distribution. Further work with spatially complete data will be needed to assess this.

Spiral structure: Spiral arms are difficult to delineate from our viewpoint within the disk. Modelling their (l, v) -traces directly is complicated by non-circular motions (Burton 1973). The most reliable information is available for the arm tangent directions of the spiral arms in the gas and young stars (see review in Englmaier & Gerhard 1999). The arm segments connecting the tangent points are more difficult to determine because of uncertain tracer distances (but see Dame *et al.* 1986). The most widely used spiral model is a four-armed pattern following Georgelin & Georgelin (1976). Such a pattern also appears most consistent with gas-dynamical models for the Milky Way (Englmaier & Gerhard 1999, Fux 1999). Much less is known about spiral arms in the old Galactic disk stars (we know from external galaxies that these need not follow the blue arms). NIR plane profiles do not clearly show all the spiral arm tangents seen in the young component (Drimmel & Spergel 2000), and the contribution of young supergiant stars to those that are seen has not been evaluated. Drimmel & Spergel (2000) conclude that both a two-armed and a sheared (relative to the gas and young stars) four-armed pattern are consistent with the DIRBE data. The best models of Fux (1999) contain four stellar spiral arms.

3. Microlensing towards the Galactic bulge

Several hundred microlensing events have now been observed towards the Galactic bulge. These observations give information about the integrated mass density towards the survey fields as well as about the lens mass distribution. The most robust observable is the total optical depth averaged over the observed fields, τ . Early measurements gave surprisingly high values $\tau_{-6} \simeq 2 - 4$ (Udalski *et al.* 1994, Alcock *et al.* 1997), where $\tau_{-6} \equiv \tau/10^{-6}$. For clump giant sources only, which do not suffer from blending problems, Alcock *et al.* (1997) inferred $\tau_{-6} = 3.9_{-1.2}^{+1.8} \times 10^{-6}$ from 13 events centered on $(l, b) = (2.55^\circ, -3.64^\circ)$. Using a difference image analysis (DIA), Alcock *et al.* (2000a) recently measured $\tau_{-6} = 2.43_{-0.38}^{+0.39}$ for all sources from 99 events centered on $(l, b) = (2.68^\circ, -3.35^\circ)$, and from this measurement deduced for the same direction $\tau = (3.23 \pm 0.5) \times 10^{-6}$ for bulge sources only. Finally, in a preliminary analysis of 52 clump giant sources in 77 Macho fields, Popowski *et al.* (2000) found a lower $\tau_{-6} = 2.0 \pm 0.4$ centered on $(l, b) = (3.9^\circ, -3.8^\circ)$.

It has long been known that axisymmetric models predict $\tau_{-6} \simeq 1 - 1.2$, insufficient to explain the quoted optical depths (Kiraga & Paczynski 1994, Evans 1994). Models with a nearly end-on bar as described in §2 enhance τ because of the longer average line-of-sight from lens to source. The maximum

effect occurs for $\phi \simeq \arctan(b/a)$ when $\tau_{\text{bar}}/\tau_{\text{axi}} \simeq (\sin 2\phi)^{-1} \simeq 2$ for $\phi = 15^\circ$ (Zhao & Mao 1996). In addition, τ increases with the mass and the length of the bar/bulge.

Even so, models based on barred mass distributions derived from Milky Way observations (§2) typically give $\tau_{-6} \simeq 1 - 2$ (e.g., Zhao, Spergel & Rich 1995, Stanek *et al.* 1997, Bissantz *et al.* 1997), significantly less than most of the measured optical depths. The new bar model of Bissantz & Gerhard (2000) gives $\tau_{-6} = 1.2$ for all sources at the position of the DIA measurement and $\tau_{-6} = 1.3$ for clump giant sources at the centroid position given by Popowski *et al.* (2000). The mass normalization of the disk and bulge in this model is calibrated by assuming constant L-band mass-to-light ratio and by matching the predicted gas flow velocities in a hydrodynamic simulation to the Galactic terminal velocity curve. As Fig. 1 shows, the apparent magnitude distributions for clump giant stars predicted by this model agree closely with those measured by Stanek *et al.* (1997). Thus the model gives a good approximation to the distribution of microlensing sources. The quoted optical depths are therefore hard to change unless one assumes that the mass distribution of the lenses differs substantially from that of the sources.

Notice that the preliminary new MACHO clump giant optical depth is within 1.7σ of the prediction of this bar model. If this clump giant optical depth is confirmed, this would be an important step in reconciling galactic structure and microlensing observations and would enable us to start using more detailed microlensing observables as constraints on Galactic models. On the other hand, the recent DIA value is still some 3.2σ away from the model prediction. While the NIR model prediction could be slightly increased if the mass-to-light ratio were not spatially constant, this is only a $\sim 20\%$ effect since limited by the terminal velocity curve (Bissantz *et al.* 1997). Recently, Binney, Bissantz & Gerhard (2000) have used general arguments to show that an optical depth for bulge sources as large as derived by the MACHO collaboration from the DIA value is very difficult to reconcile with measurements of the rotation curve and local mass density, even for a barred model and independent of whether mass follows light. To illustrate this, the extra optical depth required corresponds to an additional mass surface density towards the bulge of some $2000 M_\odot/\text{pc}^2$, comparable to that in the model of Bissantz & Gerhard (2000). Is it possible that the DIA measurement is still significantly affected by blending?

Independent of the resolution of this problem, these results have a further important implication. For, determining the mass normalization of the Bissantz & Gerhard (2000) model from the terminal velocities implicitly assumes a maximal disk. Because the predicted microlensing optical depths are if anything low, as much microlensing matter is needed within the solar circle as possible. On the other hand, little of the halo dark matter causes microlensing (Alcock *et al.* 2000b), so we can not afford significantly more dark mass inside the solar circle in the form of CDM particles, say, than corresponding to this maximum disk model. Thus the microlensing results argue strongly for a maximum disk.

4. The maximum disk and local surface density of the Milky Way

Englmaier & Gerhard (1999) computed a number of gas flow models in the gravitational potential of the NIR COBE model determined by BGS, assuming a constant joint NIR mass-to-light ratio Υ_L for the bulge and disk. The actual value of Υ_L can be specified a posteriori. For a maximum disk model it is determined by fitting the model terminal curves to the observed HI and CO terminal velocities. Some of the models included an additional dark component to prevent the outer rotation curve from falling, leading to higher circular velocities at R_0 . It turns out that the fitted value Υ_L is insensitive to the circular velocity V_0 of the Sun implied by the model: within this class of models, the mass of the disk and bulge are fixed to within $\sim 10\%$. The luminous component in these models accounts for the terminal velocities out to $|l| \simeq 45^\circ$, or $R \simeq 5.5 \text{ kpc} \simeq 2R_D$ if $V_0 = 220 \text{ km s}^{-1}$, and out to R_0 if $V_0 = 180 \text{ km s}^{-1}$.

These maximum disk models predict a surface mass density $\Sigma_\odot = 45 \text{ M}_\odot / \text{pc}^2$ near the Sun at $R_0 = 8 \text{ kpc}$ for a local circular velocity of $v_0 = 208 - 220 \text{ km s}^{-1}$. For comparison, the local surface density of ‘identified matter’ is $48 \pm 9 \text{ M}_\odot / \text{pc}^2$ (Kuijken & Tremaine 1991, Flynn & Fuchs 1994, Holmberg & Flynn 2000). Of this about $23 \text{ M}_\odot / \text{pc}^2$ is in gas and brown and white dwarfs, which contribute most to the uncertainty. That the observed and predicted surface density approximately agree lends support to the conclusion that the Galaxy indeed has a near-maximum disk; the combined observational and model uncertainty is about 30% in mass. A NIR disk accounting for only 60% of the rotation velocity at $2R_D$, as advocated for spiral galaxies by Rix & Courteau (1999), would have only $\Sigma_\odot \simeq 16 \text{ M}_\odot / \text{pc}^2$. Turned around, if the NIR disk and bulge are given the Υ_L value implied by the local surface density measurement, then they account for the observed terminal velocities in the inner Galaxy. Compared to earlier analyses, the main difference is the short disk scale-length (2.5 kpc in the model of BGS; see also Sackett 1997) – the Sun is well beyond the maximum in the rotation curve from only NIR luminous matter.

When a cored spherical halo is added to the maximum NIR disk, such as to make the Galaxy’s rotation curve approximately flat at $v_c = 220 \text{ km s}^{-1}$, the halo core radius comes out $R_c \simeq 15 \text{ kpc}$. This shows that the Milky Way’s dark halo is not very strongly concentrated. Integrating the surface density of this halo between $z = \pm 1.1 \text{ kpc}$ gives $\Sigma_{h,1.1} = 16 \text{ M}_\odot / \text{pc}^2$. Adding this to the surface density of the old NIR disk and the thick disk ($\simeq 9 \text{ M}_\odot / \text{pc}^2$, see discussion in G99), the total is $\Sigma_{\text{NIR}} + \Sigma_{\text{th}} + \Sigma_{h,1.1} = 71 \text{ M}_\odot / \text{pc}^2$, whereas the measured total $\Sigma_{1.1} = 71 \pm 6 \text{ M}_\odot / \text{pc}^2$ (Kuijken & Gilmore 1991). This very good agreement is clearly better than one expects, given the uncertainties in both numbers. Note that for smaller values of the Galaxy’s asymptotic rotation velocity, the required amount of halo would be reduced; recall that for $v_c = 180 \text{ km s}^{-1}$ the terminal velocity curve can be fitted within the errors without any added halo (at the prize of a falling rotation curve). A more detailed analysis and comparison with cosmologically motivated Milky Way halos is clearly needed.

References

Alcock C., *et al.*, 1997, ApJ, 479, 119

- Alcock, C., et al. 2000a, ApJ, 541, 734
Alcock, C., et al. 2000b, ApJ, 542, 281
Binney, J.J., Bissantz N., Gerhard, O.E., 2000, ApJL, 537, L99
Binney, J.J., Gerhard, O.E., & Spergel, D.N. 1997, MNRAS, 288, 365 (BGS)
Binney, J.J., Gerhard, O.E., Stark, A.A., et al., 1991, MNRAS, 252, 210
Bissantz, N., Englmaier, P., Binney, J.J., & Gerhard, O.E. 1997, MNRAS, 289, 651
Bissantz, N., & Gerhard, O.E. 2000, MNRAS, to be submitted
Blitz L., Spergel, D., 1991, ApJ, 379, 631
Burton W.B., 1973, PASP, 85, 679
Courteau S., Rix H.-W., 1999, ApJ, 513, 561
Dame T.M., Elmegreen B.G., Cohen R.S., Thaddeus P., 1986, ApJ, 305, 892
Dehnen W., 2000, AJ, 119, 800
Drimmel R., Spergel D.N., 2000, ASP, in press, astro-ph/0008313
Dwek E., *et al.*, 1995, ApJ, 445, 716
Englmaier, P. & Gerhard, O.E. 1999, MNRAS, 304, 512
Evans N.W., 1994, ApJL, 437, L31
Flynn C., Fuchs B., 1994, MNRAS, 270, 471
Freudenreich H.T., 1998, ApJ, 492, 495
Fux R. 1999, A&A, ,, 345,787
Georgelin Y.M., Georgelin Y.P., 1976, A&A, 49, 57
Gerhard O.E., 1999, in Galaxy Dynamics, ASP, 182, 307 (G99)
Hammersley P.L., Cohen M., Garzón F., et al., 1999, MNRAS, 308, 333
Hammersley P.L., Garzón F., Mahoney T.J., et al., 2000, MNRAS, 317, L45
Holmberg, J., & Flynn, C. 2000, MNRAS, 313, 209
Kent S.M., Dame T.M., Fazio G., 1991, ApJ, 378, 131
Kiraga M., Paczyński B., 1994, ApJ, 430, L101
Kuijken K., Gilmore G., 1991, ApJ, 367, L9
López-Corredoira M., Garzón F., Hammersley P.L., et al., 1997, MNRAS, 292, L15
López-Corredoira M., Hammersley P.L., Garzón F., et al., 2000, MNRAS, 313, 392
Nikolaev S., Weinberg M.D., 1997, ApJ, 487, 885
Ortiz R., Lépine J.R.D., 1993, A&A, 279, 90
Popowski P., et al., 2000, ASP, in press, astro-ph 0005466
Robin A.C., Crézé M., Mohan V., 1992, A&A, 265, 32
Sackett P.D., 1997, ApJ, 483, 103
Sevenster M.N., 1999, MNRAS, 310, 629
Stanek K.Z., et al. 1997, ApJ, 477, 163
Udalski A. *et al.*, 1994, Acta Astron., 44, 165
Unavane M., Gilmore G., 1998, MNRAS, 295, 145
van Loon J.T., 2000, ASP, in press, astro-ph/00009471
Weiland J.L., *et al.*, 1994, ApJL, 425, L81
Weiner B., Sellwood J.A., 1999, ApJ, 524, 112
Zhao H.S., 2000, MNRAS, 316, 418
Zhao H.S., Mao S., 1996, MNRAS, 283, 1197
Zhao H.S., Spergel D.N., Rich R.M., 1995, ApJ, 440, L13